Glycoengineered nanoparticles enhance the delivery of 5-fluoroucil and paclitaxel to gastric cancer cells of high metastatic potential

Elisabete Fernandes, Dylan Ferreira, Andreia Peixoto, Rui Freitas, Marta Relvas-Santos, Carlos Palmeira, Gabriela Martins, Anabela Barros, Lúcio Lara Santos, Bruno Sarmento, José Alexandre Ferreira

PII: S0378-5173(19)30691-X
DOI: https://doi.org/10.1016/j.ijpharm.2019.118646
Reference: IJP 118646

To appear in: *International Journal of Pharmaceutics*

Received Date: 1 July 2019
Revised Date: 26 July 2019
Accepted Date: 24 August 2019

Please cite this article as: E. Fernandes, D. Ferreira, A. Peixoto, R. Freitas, M. Relvas-Santos, C. Palmeira, G. Martins, A. Barros, L.L. Santos, B. Sarmento, J.A. Ferreira, Glycoengineered nanoparticles enhance the delivery of 5-fluoroucil and paclitaxel to gastric cancer cells of high metastatic potential, *International Journal of Pharmaceutics* (2019), doi: https://doi.org/10.1016/j.ijpharm.2019.118646

Glycoengineered nanoparticles enhance the delivery of 5-fluoroucil and paclitaxel to gastric cancer cells of high metastatic potential

Elisabete Fernandes[a,b,c,d,e*], Dylan Ferreira[a,e,*], Andreia Peixoto[a,b,c,d], Rui Freitas[a,g] Marta Relvas-Santos[a,e], Carlos Palmeira[a,h,i], Gabriela Martins[h], Anabela Barros[e,j], Lúcio Lara Santos[a,b,e,l,m], Bruno Sarmento[c,d,n], José Alexandre Ferreira[a,b,m]

[a]Experimental Pathology and Therapeutics Group, Portuguese Institute of Oncology, 4200-162 Porto, Portugal; [b]Institute of Biomedical Sciences Abel Salazar (ICBAS), University of Porto, 4050-013 Porto, Portugal; [c]Institute for Research and Innovation in Health (i3s), University of Porto, 4200-135 Porto, Portugal; [d]Institute for Biomedical Engineering (INEB), Porto, Portugal, 4200-135 Porto, Portugal; [e] Digestive Cancer Research Group, 1495-161 Algés, Portugal; [f]Faculty of Medicine, University of Porto, 4200-319 Porto, Portugal; [i]QOPNA, Department of Chemistry, University of Aveiro, 3810-193 Aveiro, Portugal; [s]QOPNA, Department of Chemistry, University of Aveiro, 3810-193 Aveiro, Portugal; [h]Immunology Department, Portuguese Institute of Oncology of Porto, 4200-162 Porto, Portugal; [i]Health Science Faculty, University of Fernando Pessoa, 4249-004 Porto, Portugal; [j]Department of Medical Oncology, Coimbra Hospital and University Centre, 3075-075 Coimbra, Portugal; [l]Department of Surgical Oncology, Portuguese Institute of Oncology of Porto, 4200-162 Porto, Portugal; [m]Porto Comprehensive Cancer Centre (P.ccc), 4200-162 Porto, Portugal; [n]Institute of Research and Advanced Training in Health Sciences and Technologies (CESPU) 4585-116, Gandra PRD, Portugal.

*Equal contribution

Corresponding author:

José Alexandre Ferreira (jose.a.ferreira@ipoporto.min-saude.pt)
Experimental Pathology and Therapeutics Group, Research Centre, Portuguese Oncology Institute of Porto, R. Dr. António Bernardino de Almeida 62, 4200-162 Porto, Portugal; Tel. +351 225084000 (ext. 5111).

Abstract

Gastric cancer is the third leading cause of cancer-related death worldwide, with half of patients developing metastasis within 5 years after curative treatment. Moreover, many patients cannot tolerate or complete systemic treatment due severe side-effects, reducing their effectiveness. Thus, targeted therapeutics are warranted to improve treatment outcomes and reduce toxicity. Herein, poly(lactic-co-glycolic acid) (PLGA) nanoparticles loaded with 5-fluorouracil (5-FU) and paclitaxel were surface-functionalized with a monoclonal antibody targeting sialyl-Lewis A (sLeA), a known glycan mediating hematogenous metastasis.

Nanoparticles, ranging from 137 to 330 nm, enabled the controlled release of cytotoxic drugs at neutral and acid pH, supporting potential for intravenous and oral administration. Nanoencapsulation also reduced the initial toxicity of the drugs against gastric cells, suggesting it may constitute a safer administration vehicle. Furthermore, nanoparticle functionalization significantly enhanced targeting to sLeA cells *in vitro* and *ex vivo* (over 40% in comparison to non-targeted nanoparticles). In summary, a glycoengineered nano-vehicle was successfully developed to deliver 5-FU and paclitaxel therapeutic agents to metastatic gastric cancer cells. We anticipate that this may constitute an important milestone to establish improved targeted therapeutics against gastric cancer. Given the pancarcinomic nature of the sLeA antigen, the translation of this solution to other models may be also envisaged.

Keywords: Gastric Cancer; Targeted Therapeutics; Drug Delivery; Poly(lactic-co-glycolic acid) Nanoparticles; Sialyl Lewis A.

1. Introduction

Gastric cancer is the third leading cause of cancer-related death worldwide, with an estimated 783,000 deaths in 2018 (Rawla and Barsouk, 2019). Locally advanced tumours are commonly subjected to repeated cycles of chemotherapy to reduce tumor size, risk of metastization and control disease dissemination (Park and Chun, 2013). However, half of patients develop metastasis within 5 years after curative treatment and many cannot tolerate or complete systemic treatment due to severe treatment side-effects, which may include neuropathy, cardiopathy, immune depression and many other severe outcomes (Park and Chun, 2013). Chemotherapy for gastric cancer frequently includes the intravenous administration of formulations containing 5-fluorouracil (5-FU), a fluorinated pyrimidine uracil analog whose mechanism of action is not yet fully understood (Sastre et al., 2006). Notwithstanding, it is known that 5-FU requires multiple conversions to form active metabolites, with the main cytotoxic activity being associated to thymidylate synthase binding and inhibition, ultimately interfering with nucleic acids synthesis (Zhang et al., 2008). Taxanes, particularly paclitaxel, have also emerged as important chemotherapeutic agents (Salati et al., 2017). Paclitaxel targets the tubulin beta-subunit of microtubules, promoting defects in mitotic spindle assembly, chromosome segregation, and ultimately cell division (Steinmetz and Prota, 2018). Furthermore, it induces Bcl-2 phosphorylation, triggering apoptosis (Pathan et al., 2001). Although highly efficient against the tumour bulk it is also extremely hydrophobic, significantly limiting its solubilization and intravenous administration, urging the introduction of alternative and more effective delivery vehicles (Kalepu and Nekkanti, 2015). In summary, despite upfront improvements in patient survival, the efficacy of these chemotherapy agents for gastric cancer is constantly challenged by significant intra-tumoral clonal heterogeneity associated to multiple intrinsic and acquired resistance mechanisms and dose-limiting side-effects (Marin et al., 2016). Thus, targeted therapeutics are warranted to improve treatment outcomes and reduce toxicity. Particular emphasis should be set on enhancing drug delivery to sub-populations of cancer cells showing higher metastatic potential, which are ultimately responsible for disease progression and dissemination (Ferreira et al., 2016). Nanoscale drug delivery vehicles have improved the efficacy of chemotherapeutic agents, with several formulations being available for different tumor types (Senapati et al., 2018). Namely, nanoparticles (NPs) for drug delivery increase the

circulation time of the conjugated or entrapped therapeutic drugs by exploiting the tortuous and poorly differentiated vasculature of solid tumors that, in contrast to healthy tissues, allow the extravasation of drugs with sizes up to several hundred nanometers (Greish, 2007). Solid tumors also lack functional lymphatic systems, making them unable to eliminate nanomaterials. Consequently, long-circulating nanomedicines tend to accumulate in tumors over time, a mechanism known as enhanced permeability and retention effect (Golombek et al., 2018; Matsumura and Maeda, 1986). Moreover, nanomedicines have improved the pharmacokinetics and efficacy of bioactive agents, while reducing systemic toxicity (Adjei et al., 2018; Patra et al., 2018); nevertheless, few studies explored their potential to treat gastric cancer in comparison to other models (Fernandes et al., 2015). In particular, poly(lactic-co-glycolic acid) (PLGA) is one of the most biocompatible polymers for NPs formulation envisaging controlled drug release. Its attractive properties include: (i) biodegradability and biocompatibility; (i) well established formulations and production methods adapted to various types of small or macromolecules of either hydrophilic or hydrophobic nature; (ii) approval by EMA and FDA, (iv) protection of drugs from degradation, (v) controlled release, (vi) possibility to graft the surface with different functional groups and/or biomolecules capable of providing stealthiness and/or improving interaction with biological materials/milieus and (vii) possibility to target NPs to specific cells and organs, significantly improving its efficiency (Martins et al., 2018). Namely, PLGA NPs surface has been functionalized with antibodies and antibody fragments targeting relevant cancer-associated antigens such as CEA, HER2, and CD44 (Dominguez-Rios et al., 2019; Kennedy et al., 2018; Pereira et al., 2018), ultimately demonstrating that antibody-functionalization potentiates the affinity of nanomedicines to cancer cells and significantly increases its retention in tumours. Therefore, given the careful choice of the target ligand, the development of more effective target-driven nanotherapeutics for gastric cancer may be feasible.

Malignant transformation is accompanied by significant alterations in cell surface glycosylation holding tremendous potential for cancer detection and targeted therapeutics (Peixoto et al., 2019; Pinho and Reis, 2015). It has been long described that advanced stage gastric tumors and its metastasis overexpress the sialyl-Lewis A (sLeA; CA19-9) antigen, a terminal epitope of glycan chains in proteins and lipids (Trinchera et al., 2017). The sLeA antigen mediates the adhesion of cancer cells to P- and E-selectin on endothelial cells, facilitating their intravasation into the bloodstream,

dissemination and homing to distant locations (Peixoto et al., 2019; Trinchera et al., 2017). Furthermore, patients presenting strong sLeA expression are at greater risk of developing distant metastasis and the presence of this antigen has been frequently observed in gastric metastasis (Schultz et al., 2012; Zhu et al., 2018). Moreover, since the sLeA antigen is present at the cell-surface, thus easily accessible to antibodies, it constitutes an ideal target for drug delivery. As such, the present work devotes to the development of a novel biocompatible PLGA-based nanoparticle targeting aggressive sLeA positive gastric cancer cells to deliver safely chemotherapy, according tumour staging and patient performance status.

2. Material and Methods

2.1. Materials

The human gastric cancer cell line NCI-N-87 isolated from a liver metastasis and the gastric adenocarcinoma cell line AGS were purchased from ATCC. Cell culture materials included RPMI 1640+GlutaMAX™-I and OptiMEM medium, heat-inactivated FBS, and penicillin-streptomycin solution from Gibco, Life Technologies. The fructosyltransferase inhibitor 2-fluoro-L-fucose (2FF) was purchased from Santa Cruz Biotechnology. 3-(4,5-dimethylthiazol-2-yl)-2,5-diphenyltetrazolium bromide (MTT) was acquired from ThermoFisher Scientific. The surfactant Triton X-100, the fixative paraformaldehyde (PFA) and dimethyl sulfoxide (DMSO) were acquired from Sigma-Aldrich. Cytotoxic drugs 5-FU and Paclitaxel were acquired from Sigma-Aldrich and Indena S.p.A, respectively. Reagents for nanoparticle preparation, such as ethyl acetate, pluronic F-127, acetone, 1-ethyl-3(3-dimethylaminopropyl)carbodiimide (EDC), N-hydroxysuccinimide (NHS), 2-(N-morpholino)ethanesulfonic acid (MES), Coumarin-6 (C6) and sodium chloride were purchased to Sigma-Aldrich. Furthermore, 50:50 (Lactide:Glycolide) - Poly(Lactide-co-Glycolide) (PLGA) was provided by Corbion Biomaterials. Supernatants quantification was achieved using the Quick Start Bradford 1 x Dye Reagent from BioRad. Antibodies for nanoparticle functionalization and cellular staining, such as anti-sLeA monoclonal antibody [CA19-9-203] and mouse IgG1 [MOPC-21] isotype control were provided by Abcam, while the polyclonal rabbit anti-mouse immunoglobulins/FITC secondary antibody was provided by DAKO. CellMask™ Orange 0.5x cell staining was acquired from Invitrogen. Enzymatic controls as Neuraminidase from *Clostridi*um *perfringens* and PNGase F from

Elizabethkingia meningoseptica were provided by Sigma-Aldrich. Tissue sections analysis was achieved using the Novolink Max Polymer DS Kit from Leica and citrate buffer from Vector.

2.2. Nanoparticle Production, Functionalization and Characterization

2.2.1. Nanoparticles Production

NPs containing 5-Fluoruracil (5-FU, Sigma-Aldrich) were generated by a modified water-in-oil-in-water (w/o/w) double emulsion-solvent evaporation technique (Gomes et al., 2017; Sousa et al., 2017). Briefly, 30 mg of 50:50 (Lactide:Glycolide) - Poly(Lactide-co-Glycolide) (PLGA, Corbion-Purac Biomaterials) was dissolved in 4mL ethyl acetate (Sigma-Aldrich), following the addition of 10mg/mL 5-FU and emulsification at 70% amplitude for 30s using a Vibra-Cell™ ultrasonic processor in an ice bath. The second emulsion was achieved by adding 2% Pluronic F-127 (6mL) (Sigma-Aldrich) to the first emulsion, following Vibra-Cell™ ultrasonic homogenization for 60s and addition of the resulting mixture to 12mL of the same surfactant. Ethyl acetate evaporation from the final solution occurred for 5h under magnetic stirring at 250 rpm. Nanoparticles were isolated by centrifugation at 120 000 *g* for 40 min. Paclitaxel NPs were produced through a modified nanoprecipitation method (Fessi et al., 1989). Accordingly, 30 mg PLGA was dissolved in acetone (Sigma-Aldrich) and added to 10 mg paclitaxel (Indena S.p.A). This organic solution was transferred through a 25 G needle to an aqueous solution of 1% Pluronic F-127 (15 mL) and solvent evaporations occurred under magnetic stirring at 250 rpm for 3h. A washing step with Milli-Q water was performed. Fluorescent PLGA NPs loaded with Coumarin-6 (C6) (Sigma-Aldrich) were obtained using the same methodology but dissolving 0.8 mg of C6 in acetone.

2.2.2. Nanoparticles functionalization with the anti-sLeA antibody

PLGA NPs were covalently functionalized with an anti-sLeA monoclonal antibody (CA19-9-203, ab222370, Abcam) following the carbodiimide chemistry for bioconjugation (Pereira et al., 2018). The coupling reaction was carried out in the presence of 1-ethyl-3(3-dimethylaminopropyl)carbodiimide (EDC) and N-

hydroxysuccinimide (NHS) (Sigma-Aldrich) allowing the carboxyl-terminated NPs to react with the primary amine of the antibody, yielding an amide bond. PLGA NPs were then centrifugated at 10,000*g* for 20 min and resuspended in 0.1M 2-(N-morpholino)ethanesulfonic acid (MES) (Sigma-Aldrich) pH 5.5. For NPs activation step, 1mL 0.1M EDC and 1mL 0.7M NHS were added dropwise to the previous NP suspension, which was kept 1h at room temperature under agitation in the dark. To remove excess EDC/NHS, PLGA NPs were centrifuged and resuspended in PBS pH 7.4 at a final concentration of 2 mg/mL. Activated NPs were then conjugated with 150µg anti-sLeA moAb at 4°C overnight, centrifuged at 10,000*g* for 10min and re-dispersed in PBS at a final concentration of 4 mg/mL. The supernatants were stored for further antibody quantification by the Bradford method following the Quick Start Bradford 1 x Dye Reagent assay procedure (BioRad). The percentage of conjugation efficiency was determined according to the following equation:

$$\text{Conjugation efficiency (\%)} = \frac{\text{amount of inputed moAb} - \text{amount of antibody in supernatant}}{\text{amount of inputed moAb}} \text{x100}$$

In addition, the functionalization of PLGA NPs was evaluated by Fourier Transform Infrared Spectroscopy (FTIR) using an ABB MB3000 FTIR spectrometer (ABB) equipped with a MIRacle single reflection attenuated total reflectance (ATR) accessory (PIKE Technologies). For each NPs spectrum, a scan was collected in the mid- infrared region (3,600–600 cm^{-1}). Spectral analysis was executed using the Horizon MB™ FTIR software (ABB).

2.2.3. Nanoparticles physicochemical and morphological characterization

The size and polydispersity index (PdI) of formulations were determined by Dynamic Light Scattering (DLS), while surface charge of NPs was determined by laser Doppler anemometry (LDA). After dispersion, NPs were diluted in 10 mM sodium chloride solution (pH 7.0) (Sigma-Aldrich) and DLS and LDA were performed with a Nano ZS Zetasizer (Malvern, Worcestershire, UK) at 25°C. Surface morphology and NPs size confirmation were performed by transmission electron microscopy (TEM) using a JEM-1400 microscope (JEOL, Tokyo, Japan) at an acceleration voltage of 80 kV.

2.3. Nanoparticles loading and controlled drug release

2.3.1. Association efficacy and drug loading

Supernatants of different formulations were analyzed by high-performance liquid chromatography (HPLC, Shimadzu UFLC Prominence System) to determine the association efficiency of 5-FU and Paclitaxel into PLGA NPs. The chromatographic conditions for 5-FU quantification included a Waters column with a guard column pumped at a flow rate of 0.5mL/min. The mobile phase was composed of acetonitrile and water (5:95, *v/v*) and the volume of sample injected was 10µl. The PDA detection wavelength was 265 nm with a run time of 7min at 20°C. The chromatographic conditions for Paclitaxel quantification were previously described by (Pereira et al., 2018). The Association Efficacy (AE) and Drug Loading (DL) were determined using the following equations:

$$AE\ (\%) = \frac{\text{Initial mass of drug} - \text{Mass of drug in supernatant}}{\text{Total mass of drug}} x100$$

$$DL\ (\%) = \frac{\text{Initial mass of drug} - \text{Mass of drug in supernatant}}{\text{Theoretical mass of nanoparticles}} x100$$

2.3.2. 5-FU and paclitaxel controlled release

Envisaging both oral and intravenous administration of nanoformulations, the release profiles of 5-FU or Paclitaxel-loaded PLGA-NPs were determined in PBS and PBS 1% pluronic, respectively, at physiological pH 7.4 and gastric pH 3.5 under agitation at 37°C. Briefly, 500µl of NPs suspensions supernatant were removed at 0.25, 0.5, 1, 2, 4, 6, 8, 12, 24, 32, 48, 56, and 72h and replaced with the same amount of respective buffer. The supernatants were centrifuged at 10,000*g* for 20min and quantified by HPLC as previously described.

2.4. Functionalized nanoparticles evaluation in gastric cancer cell models

2.4.1. Cell culture conditions

The human gastric cancer cell line NCI-N-87 isolated from a liver metastasis and the gastric adenocarcinoma cell line AGS were purchased from ATCC and cultured with RPMI 1640+GlutaMAX™-I medium (Gibco, Life Technologies), supplemented with 10% heat-inactivated FBS (Gibco, Life Technologies) and 1% penicillin-streptomycin (10,000 Units/mL penicillin; 10,000 mg/mL streptomycin; Gibco, Life Technologies). Cell lines were cultured as a monolayer at 37°C in a 5% CO_2 humidified atmosphere and were routinely subcultured after trypsinization. For internalization assays, 500 µM 2-fluoro-L-fucose (2FF, Santa Cruz Biotechnology) were added to NCI-N-87 cell culture medium for 24h to selectively inhibit fucosylation and consequently sLeA levels at the cell-surface. This inhibition provided a negative control for *in vitro* PLGA-sLeA NPs internalization assays.

2.4.2. Evaluation of sLeA expression in gastric cancer cell models

PFA-fixed NCI-N-87 and AGS cells were screened for sLeA using a 1:100 dilution of the anti-sLeA [CA19.9-9-203] monoclonal antibody (ab116024, Abcam) in PBS 2% FBS for 1h at room temperature. Experiments using a mouse IgG1 [MOPC-21] Isotype Control (ab18443, Abcam) were included as negative controls. Polyclonal rabbit anti-mouse immunoglobulins/FITC (DAKO; F0313) was used as secondary antibody. Other experimental controls included the overnight digestion of whole cells with 10 mU/mL Neuraminidase from *Clostridium perfringens* (Sigma-Aldrich) or 25mU/mL PNGase F from *Elizabethkingia meningoseptica* (Sigma-Aldrich) prior to flow cytometry analysis. PNGase F digestion contributed to disclosing the contribution of *N*-glycans for sLeA expression on glycoproteins. Both controls consisted in overnight enzymatic digestion of $1x10^6$ cells at 37°C under mild agitation. Two independent experiments were performed in triplicate for each cell line and condition. At least 20 000 events were acquired for each condition using a FC500 (Beckman Coulter) cytometer and data analysis was performed through InfinicytTM (Cytognos) Software.

2.4.3. Nanoparticles cytotoxicity profiles

The cytotoxicity of free drugs (5-FU and paclitaxel) and functionalized NPs loaded with chemotherapy were determined using MTT assay. Accordingly, gastric cancer cell lines NCI-N-87 and AGS were seeded into 96 well plates at a cell density of 40 000 and 10 000 cells/well, respectively, and exposed to increasing doses of free drugs and NPs

formulations. After 24h exposure, conditioned media was replaced by 100µl fresh culture medium and 10 µL of a 12 mM 3-(4,5-dimethylthiazol-2-yl)-2,5-diphenyltetrazolium bromide (MTT, ThermoFisher Scientific) stock solution was added to each well, following a 4h incubation at 37°C in a humidified chamber. 75 µl of conditioned medium was removed from the wells and 50 µL of DMSO (Sigma-Aldrich) was added to solubilize formazan crystals. Plates were incubated at 37°C for 10 minutes and absorbances were read at 540 nm in a microplate spectrophotometer. Positive controls (untreated cells; empty functionalized NPs exposed cells) and a negative control (cells treated with 1% triton-X 100) were included. Thus, the metabolic activity (%) of living cells was calculated through the following the equation:

$$\text{Metabolic activity (\%)} = \frac{\text{absorbance of treated cells}}{\text{absorbance of positive control}} \text{x} 100$$

2.4.4. Nanoparticles internalization by sLeA positive gastric cancer cells

The interactions between NPs and gastric cancer cell lines (NCI-N-87 and AGS) was evaluated by fluorescence microscopy and flow cytometry, using coumarin 6 (C6)-loaded NPs. NCI-N-87 cells exposed to 2FF (as described in section 2.6) and showing reduced sLeA expression were used as negative controls. For fluorescent microscopy assays, cells were seeded in 12-well plates and incubated for 4h at 37°C with fresh medium or 1.5mg/mL PLGA NPs, PLGA NPs loaded with C6 (PLGAc), PLGAc-EDC/NHS, and PLGAc-sLeA in OptiMEM. medium. Cells were fixed with 4% PFA and stained with CellMask™ Orange 0.5x (Invitrogen) for 6min at room temperature. The uptake of fluorescent NPs was evaluated under inverted fluorescence microscopy (Leica DMI 6000 from Leica), detecting PLGAc NPs through the GFP channel and CellMask™ stained cells through TXR the channel. Tilescan analysis was performed using the LAS X software. For flow cytometry analysis, cells were incubated according to the same protocol, detached through a non-enzymatic method and fixed with 4% PFA. PLGAc-NPs functionalized with Isotype IgG1 were added as negative control and cells were acquired in a NAVIOS cytometer (Beckman Coulter) using the Infinicyt™ (Cytognos) software. At least 20 000 events were acquired in each condition.

2.5. Functionalized nanoparticles binding to gastric tumours and healthy histological sections

Formalin-fixed paraffin embedded (FFPE) tissue sections from primary gastric lesions (3 advanced stage tumours; 3 superficial tumours) and corresponding metastasis, whenever available, from patients subjected to treatment at the Portuguese Institute of Oncology of Porto (IPO-Porto) in Portugal were elected for this study. All procedures were approved by the local ethics committee under patient's informed consent. Tumour sections were screened for sLeA using the anti-sLeA [CA19.9-9-203] mouse monoclonal antibody (ab116024, Abcam) and sLeA functionalized PLGAc-NPs (PLGAc-sLeA NPs) using the polymer method. Briefly, 3µm gastric cancer and healthy tissue (skin, lung, pancreas, colon, small intestine, liver, kidney, stomach) sections were deparaffinized, rehydrated and incubated for 15min with boiling citrate buffer (Vector). Tissue sections were then exposed to 3-4% hydrogen peroxide for 5min (Leica) and sLeA was detected using the Novolink Max Polymer DS Kit (Leica) according to the manufacturer instructions. Positive and negative controls were tested in parallel. Negative controls consisted in 5% BSA devoid of primary antibody, PLGAc, PLGAc-EDC/NHS and PLGAc-Isotype NPs, while the positive control corresponded to a subsequent tissue section stained using the anti-sLeA monoclonal antibody. An additional negative control was performed with recourse to 0.2U/mL Neuraminidase from *Clostridium perfringers* (Sigma-Aldrich) overnight at 37ºC prior incubation with anti-sLeA moAb and PLGAc-sLeA.

2.6. Statistical analysis

GraphPad Prism 7 analysis was used to analyse the significance level (ANOVA with Dunnet's test) and determine the EC50 value. All experiments were performed in triplicate and represented as mean ± standard deviations (SD). A Kruskal–Wallis one-way analysis of variance (one-way non-parametric ANOVA) was used to evaluate the effect of pH on drugs-controlled release. Two-way ANOVA with Bonferroni's post hoc test (GraphPad Prism software Inc., USA) was used to analyse cytotoxicity profiles. The level of significance was set at probabilities of "*" $p < 0.05$; "**" $p < 0.01$; "***" $p < 0.001$; and "****" $p < 0.0001$.

3. Results and Discussion

The present work focusses on the development of novel biocompatible PLGA-based NPs targeting gastric cancer cells showing higher metastatic potential, translated

by the expression of cell surface sLeA antigen. The overall objective is to improve the delivery of 5-FU and paclitaxel to these cells while providing means to surpass systemic administration issues, such as indiscriminate cytotoxicity and potential off-target effects.

3.3. Physicochemical and morphological characterization of nanoparticles

PLGA NPs were produced through the double emulsion-solvent evaporation technique and modified nanoprecipitation method. Empty (controls) as well as 5-FU- and paclitaxel-loaded NPs with or without sLeA moAb functionalization using an EDC/NHS linker were constructed and analyzed according to critical physicochemical and morphological properties, such as mean size, size distribution, surface charge, association efficiency (AE) and drug loading (DL) **(Table 1)**.

Nanoparticle size, as determined by dynamic light scattering (DLS), ranged between 137 and 330 nm. Furthermore, transmission electron microscopy (TEM) confirmed the aspheric shape of NPs, as well as the size range **(Figure 1)**. The size of the NPs determines its vascular and lymph systems clearance, as such, the optimal NP size to escape accelerated elimination was approximately 100nm (Prokop and Davidson, 2008), however, manipulation of surface characteristics provided an opportunity to generate ideal systems despite the increase in size resulting from functionalization. The increased size of functionalized NPs probably resulted from the addition of EDC/NHS linkers to its surface and/or NPs aggregation, which was described as a common event derived from carbodiimide chemistry (Shen et al., 2009). In addition, FTIR analysis of functionalized NPs was performed to confirm the covalent binding of anti-sLeA moAb to PLGA-NPs **(Figure 2)**. Accordingly, at 1750 cm^{-1}, a marked peak suggested the presence of a carbonyl bond (C=O stretching vibration) characteristic of PLGA **(Figure 2A)**. Antibody covalent conjugation to the NPs *via* an EDC/NHS linker led to the appearance of an amide bond (C=N stretching vibration) at 1640 cm^{-1}. Moreover, an additional peak at 1560 cm^{-1} stood out in the PLGA-sLeA NPs spectra, corresponding to the amine groups of the moAb (N-H bending vibrations) **(Figure 2C)**. Together these findings confirm the covalent binding of the anti-sLeA moAb to PLGA NPs. Furthermore, the polydispersity index (PdI) of empty and non-functionalized NPs ensured a highly monodisperse population (<0.1), which was amplified by moAb functionalization (Hughes et al., 2015). These findings further indicate NPs aggregation

as a result of the functionalization protocol. All formulations were negatively charged and within a desirable zeta potential for nanosuspensions stability, since in the case of a combined electrostatic and steric stabilization, a minimum zeta potential of ± 20 mV is desirable (Gupta and Trivedi, 2018). Furthermore, mild negative NPs surface charges could prevent strong repulsion from the negatively charged cell membrane, while decreasing non-specific interactions and NPs spontaneous aggregation.

The association efficacy (EA) and drug loading (DL) of 5-FU and paclitaxel into PLGA-NPs was indirectly determined by HPLC. Accordingly, 5-FU EA ranged 40% while DL was around 14%. In turn, paclitaxel-loaded NPs exhibited AE values over 90% and DL around 30%. These findings are in accordance with the solubility profile of both drugs. Notably, the hydrophilicity of 5-FU increases the diffusion to the aqueous external phase during the encapsulation process, lowering its association efficiency. Contrastingly, the high hydrophobicity of paclitaxel favours encapsulation through the nanoprecipitation method, thereby enhancing AE and DL values (El-Hammadi et al., 2017).

To assess NPs functionalization, NPs formulation supernatants were analyzed by the Bradford method after anti-sLeA moAb conjugation and the percentage of conjugation efficiency (CE) was determined (**Table 1**). Accordingly, the CE of the moAb to PLGA-NPs was 67%, exceeding the expected values for the carbodiimide chemistry of immunoconjugation (Thorek et al., 2009).

Table 1. Properties of empty, non-functionalized and functionalized NPs, including the mean size, polydispersity index (PdI), surface charge, association efficacy (EA) and drug loading (DL). The values are represented as mean values ± SD (n=3).

Encapsulated Agent	Nano-construct	Size (nm)	PdI	Surface Charge (mV)	EA (%)	DL (%)	moAb CE (%)
5-FU	Empty	137±0.2	0.058±0.001	-7.1±0.5	-	-	-
	Non-functionalized	216±2.4	0.175±0.007	-1.8±0.4	40.5±2.4	14.1±0.9	-
	Non-functionalized - EDC/NHS	224±1.6	0.131±0.004	-2.9±0.5	-	-	
	Functionalized	330±5.9	0.403±0.029	-0.9±0.1	39.4±1.5	13.9±0.3	-
Paclitaxel	Empty	174±1.1	0.099±0.043	-6.3±0.5	-	-	-

	Non-functionalized	202±5.3	0.152±0.004	-4.1±0.9	96.6±1.2	32.0±0.1	-
	Non-functionalized - EDC/NHS	224±1.	0..131±0.004	-2.9±0.5	-	-	
	Functionalized	301±7.6	0.390±0.013	-0.9±0.1	90.5±1.1	29.8±0.4	-
Coumarin-6	Functionalized	328±1.0	0.491±0.061	-14.1±0.3	-	-	67±3.0

5-FU and paclitaxel release study in aqueous solution

Envisaging the intravenous but also the oral administration of nanoformulations, the release profiles of 5-FU or paclitaxel-loaded PLGA-NPs were determined by HPLC at the physiological pH 7.4 and at the gastric pH 3.5 (**Figure 3**). Both cytotoxic drugs experience a burst release in the first few hours, followed by slower and more controlled release. Moreover, at any given timepoint, 5-FU-NPs released significantly higher amounts of cytotoxic drug at pH 7.4 than at 3.5 ($p<0.001$), vowing for a pH-dependent release. Contrastingly, paclitaxel release from PLGA-NPs was not pH-dependent in this experimental setup. Furthermore, 5-FU release occurred at an accelerated pace compared to paclitaxel, which could be once again due to its hydrophobicity and resistance to diffusion to the aqueous environment. As such, PLGA-NPs may offer an opportunity for the controlled release of paclitaxel *in vivo* and support the possibility of intravenous as well as oral administration.

3.4. sLeA expression in Gastric cell lines for *in vitro* studies

Two gastric cancer cell lines of different origins, namely the human gastric adenocarcinoma cell line AGS and human gastric metastatic cell line NCI-N87 were screened for sLeA expression by flow cytometry, envisaging models for screening NPs toxicity profile and affinity. Autofluorescence, secondary antibody and IgG1 isotype controls were used to define positivity thresholds. Enzymatic negative controls using α-Neuraminidase and PNGase F, removing sialic acids from sLeA impairing antibody recognition and removing *N*-glycan chains potentially carrying sLeA, respectively, were also included. According to this analysis, the epithelial cell line AGS does not show significant sLeA expression, while metastatic NCI-N-87 cells overexpress this antigen. Furthermore, in NCI-N-87 cells, sLeA is mostly represented in *N*-glycans as demonstrated by the dramatic signal decrease upon PNGase F treatment

(**Supplementary Figure 1**). These results are consistent with other recently published studies demonstrating the increased expression of *FUT3* and ST3GAL4 genes in NCI-N-87 cells compared to AGS cells, which translates in increased terminal α1,4-linked fucosylation and α2,3-linked sialylation in terminal glycan chains, ultimately leading to sLeA overexpression (Duarte et al., 2017). Furthermore, the presence of high-levels of sLeA in NCI-N-87 cells, originally isolated from a liver metastasis, reinforces this glycan's role in P- and E-selectin mediated hematogenous dissemination (Lange et al., 2016).

3.5. Nanoparticle cytotoxicity profiles *in vitro*

The cytotoxicity of free and nanoencapsulated chemotherapy agents were determined using the metabolic MTT assay, a colorimetric assay assessing cell metabolic activity and reflecting the number of viable cells. Untreated cells and cells exposed to empty functionalized NPs (Empty NP moAb) were included as positive controls, while cells treated with 1% triton-X 100 that promotes massive cell death were included as negative control. Gastric cancer cell lines NCI-N-87 ($sLeA^+$) and AGS ($sLeA^-$) were exposed to increasing concentrations of free and targeted nanoencapsulated drugs (10 - 100 nM), including the half maximal inhibitory concentration (IC50) of both drugs (1.6 and 60 nM for 5-FU in NCI-N-87 and AGS, respectively; 7nM and 23 nM for paclitaxel in NCI-N.87 and AGS, respectively) (Samulitis et al., 2015; Wang et al., 2018; Zhang et al., 2013) (**Figure 4**). Two-way ANOVA showed that drug concentration, the type of formulation (free drug, empty functionalized NPs, antibody-NP conjugates) and the synergism of both factors contributed to influence cell viability ($p < 0.0001$), irrespectively of the cell line. Moreover, the increase in concentration of free drugs was inversely correlated with cellular viability in both cell lines. Nevertheless, AGS were more sensitive to 5-FU in comparison to paclitaxel whereas NCI-N-87 presented the opposite behaviour, denoting a cell-dependent drug response profile. However, in general, the AGS cell model was more sensitive to the tested chemotherapy agents in comparison to NCI-N-87, irrespectively of the drug. Contrastingly, nanoencapsulation significantly reduced the toxicity profile of both drugs for the two cell lines. Moreover, the fact that the NPs content had not been entirely released after 24h further reinforces the notion of controlled release provided by nanoencapsulation and may account for the lower

toxicity presented by this delivery strategy. Notably, the targeted nature of nanoencapsulated drugs did not translate into noticeable differences in cytotoxicity between cell lines at 24h, irrespectively of marked differences in sLeA expression (Figure 4). Such observations may be directly linked to the slower drug release kinetics promoted by nanoencapsulation and supported by controlled release studies. Moreover, it demonstrates that the presence of the antibody did not promote toxicity. Overall, cell viability for all nanoformulations was significantly above 70%, which is regarded as toxicity threshold according to ISO 10993-5 (Han et al., 2019), reinforcing the value of these NPs for drug delivery.

3.6. Internalization of nanoparticles by sLeA positive cells

The interactions between NPs and gastric cancer cell lines (NCI-N-87 and AGS) was evaluated by fluorescence microscopy and flow cytometry, using Coumarin 6 (C6)-loaded NPs (**Figure 5**). According to FACS analysis, functionalized NPs showed almost a 2-fold increase in affinity for NCI-N-87 cells in comparison to void NPs, NPs conjugated with the ECD/NHS linker or the IgG1 isotype control, as translated by the increased mean fluorescence intensity of coumarin-6 (**Figure 5A and B**). Contrastingly, this was not observed for AGS cells, reinforcing that the presence of the antibody significantly enhanced NPs uptake by cancer cells expressing sLeA (**Figure 5A and C**). However, studies involving non-functionalized and IgG1 isotype-functionalized particles showed significantly higher NPs concentrations in AGS in comparison to NCI-N-87. Such observations suggest that the magnitude of the targeting effect may be underestimated by the initial unselective uptake behaviour demonstrated by AGS in comparison to NCI-N-87. As such, to elucidate further on the targeted effect of NPs, NCI-N-87 cells were incubated with 2FF, a known inhibitor of fucosyltransferases responsible by sLeA biosynthesis (Zhou et al., 2017), which resulted in a 20% decrease in the total amount of cell surface antigen and a 25% decrease in NPs internalization (**Supplementary Figure 2**).

Fluorescent immunocytochemistry analysis using CellMask™ staining and Coumarin 6-labelled NPs was performed to further access NPs internalization by gastric cancer cells. NCI-N-87 cells presented a higher uptake of functionalized NPs per cell in comparison to non-functionalized controls (**Figure 5D**). The higher fluorescence intensity observed in the cytoplasm of NCI-N-87 cells exposed to functionalized NPs

also suggested an increase in NPs uptake, thus in agreement with flow cytometry analysis. Again, AGS cells displayed no differences in internalization rates. These observations reinforce that antibody functionalization improved NPs targeting to sLeA expressing cells, suggesting potential as a drug delivery vehicle for metastatic gastric cancer.

3.7. Binding of functionalized nanoparticles to gastric tumour and healthy tissues sections *ex vivo*

To disclose the *ex vivo* targetability of functionalized NPs, formalin-fixed paraffin embedded (FFPE) gastric tissue sections were first screened for sLeA by immunohistochemistry using the free antibody and functionalized NPs. Three advanced stage primary lesions and corresponding distant metastasis as well as three superficial gastric tumours were elected for this study. High levels of sLeA were observed in the tumour area of advanced cases and corresponding metastasis but not in the apparently normal adjacent mucosa (**Figure 6**). sLeA was mostly detected at the cell surface, in accordance with its typical expression pattern in human tissues (Blanas et al., 2018). In addition, low sLeA expression was observed in early stage lesions, reinforcing the aggressive nature of this molecular feature (Konno et al., 2002). Notably, sLeA was detected in all the metastasis, reinforcing its role in this process and suggesting potential for targeting disseminated disease (Blanas et al., 2018; Carrascal et al., 2018; Kannagi et al., 2004). Parallel analysis of the same sections with NPs functionalized with IgG1 isotype antibody, empty PLGA NPs and PLGA-EDC/NHS NPs showed no unspecific staining. Moreover, anti-sLeA functionalized NPs displayed a staining pattern similar to the free antibody. The specificity of NPs for cancer cells was reinforced by the existence of reactivity solely in tumour areas but not in non-neoplastic areas, including lymphoid and muscle tissues. This was further confirmed by the large reduction in NPs-mediated staining in neuraminidase treated tumour sections (data not shown). Interestingly, antibody functionalized NPs provided a more intense staining pattern compared to the free antibody, suggesting that NPs may have provided signal amplification as a result of multiple antibody conjugates per nanoparticle. Future studies should devote to disclose the potential of nanoplatforms in deciphering trace amounts of clinically relevant cancer-antigens in tumour sections. Finally, we have accessed the affinity of functionalized NPs for a panel of healthy tissue sections from 9 relevant

organs (skin, lung, stomach, small intestine, colon, liver, pancreas, kidney and lung) (**Figure 7**). Functionalized NPs did not bind to lymphoid and muscle tissues, as previously observed for gastric tumour adjacent mucosa. It also did not bind to vasculature or normal stomach epithelium, with the exception of a faint affinity for mucinous secretions known to yield high glycan density (Blanas et al., 2018; Fry et al., 2008). Moreover, NPs did not show any affinity for liver and kidney sections; nevertheless, low levels of staining could be observed in the exocrine pancreas (pancreatic acini) and in mucus-producing cells, particularly in goblet cells of the intestinal and respiratory epithelia. A faint cytoplasmatic staining could also be observed in the skin upper layers (granular and lucidium layers) but no expression was found in the other four epidermal layers. Taken together, these observations demonstrate that functionalized NPs present a restricted affinity for healthy tissues and high affinity for sLeA expressing cancer cells in *ex vivo* settings. This emphasises the potential of this nanomedicine for drug delivery in complex tissue contexts and sets the necessary molecular rational for studies *in vivo*.

4. Conclusions

Gastric cancer remains the third leading cause of cancer-related death worldwide due to difficulties controlling disease dissemination associated with the severe toxicity of chemotherapy agents, urging novel, less toxic and more effective target therapeutics. As such, the present work devoted to the development of a novel biocompatible PLGA nanoconstruct glycoengineered to target sLeA expressing gastric cancer cells. This is expected to improve the safety related with the delivery of chemotherapy to cancer cells, with emphasis on those with increased metastatic potential. Moreover, targeting the sLeA antigen, which plays a functional role in hematogenous dissemination of disease while presenting a very restricted expression pattern in healthy tissues, holds potential to reduce the off-target effects of current systemic chemotherapy. This aspect is particularly critical for improving the management of fragile gastric cancer patients unable to tolerate current chemotherapy formulations due to toxicity issues.

Envisaging this goal, we have synthesized nanoparticles with a size ranging between 137 and 330 nm upon functionalization. All formulations displayed acceptable polydispersity index and were within a desirable zeta potential for nanosuspensions

stability for future clinical applications (ref). The association efficacy of 5-FU and Paclitaxel were 40% and 90%, respectively, reflecting their dissimilar affinity for the external phase during the encapsulation processes (El-Hammadi et al., 2017). Furthermore, the conjugation efficiency of the anti-sLeA monoclonal antibody at the PLGA-NPs surface was 67%, exceeding previous reports exploiting carbodiimide chemistry for immunoconjugation (Thorek et al., 2009).

We have then accessed the controlled release of the two nanoencapsulated drugs at physiological and acid pH, envisaging venous and oral administrations. Accordingly, 5-FU diffusion into solution was favoured by the physiological pH, while paclitaxel was found not to be pH-dependent. In addition, 5-FU release occurred at an accelerated pace compared to Paclitaxel but none of the cytotoxic agents was fully transferred to solution after 24h. As such, PLGA-NPs may offer an opportunity for the controlled release of both therapeutic agents *in vivo*.

For studies *in vitro* we elected the AGS and NCI-N-87 gastric cancer cell lines, presenting distinct molecular and pathological natures (ref, ref). Flow cytometry analysis revealed striking differences regarding sLeA expression. Namely, epithelial AGS cells did not express sLeA, while the hepatic type metastatic NCI-N-87 cells overexpressed the antigen. These findings were supported by previous reports describing that NCI-N-87 cells overexpress key glycosyltransferases responsible by sLeA overexpression (Duarte et al., 2017). It is also consistent with the origin of NCI-N-87 cells (liver metastasis) as well as the sLeA antigen functional role in metastasis development (ref,ref). These cell lines were first used to compare the cytotoxicity of encapsulated drugs with the free agents for a short initial exposure periods (24h). These assays demonstrated that nanoencapsulation significantly reduced the toxicity of both drugs due to the controlled release effect provided by the biocompatible polymer. Such observations are also in agreement with previous reports, supporting the excellent protective properties of nanoencapsulation and its potential for reducing the toxicity of different types of drugs (referenciar o reviewer e mais um ou outro artigo, pode ser o do Bruno). This is particularly important to support the development of safer drug delivery systems. Toxicity assays *in vivo* are now required to set the rational for clinical translation. Moreover, in internalization assays *in vitro*, functionalized NPs demonstrated higher affinity for sLeA expressing cells, supporting the relevance of antibody functionalization. This was later confirmed by *ex vivo* assays in gastric tumours and healthy tissues, emphasising the potential of this nanomedicine for drug

delivery given its significant affinity to cancer cells compared to healthy tissues. Future studies should now focus on translating these findings into pre-clinical tests in relevant animal models, namely by exploiting patient derived xenografts. Emphasis should also be set on disclosing the nature of the glycoproteins carrying the sLeA envisaging the design of even more specific ligands for cancer cells. Finally, given the pancarcinomic nature of the sLeA antigen we anticipate that the success of this approach might be translatable to other tumour types, including pancreas (Engle et al., 2019), breast (Hermann et al., 2017; Jeschke et al., 2005), oesophageal (Scarpa et al., 2015), colorectal (Stiksma et al., 2014; Vanderbeck and Voutsadakis, 2016), bladder (Santos et al., 2014) and other types of solid cancers.

Author Contributions

EF and DF acquired data; EF, DF, AP, CP and JAF analysed and interpreted data; RF and MRS produced the artwork; EF, DF, AP, GM, LLS and JAF drafted the article and critically revised it; EF, DF, AP, AB, LLS and JAF approved the final version of the draft to be submitted. JAF and BS conceptualized and design the study.

Conflict of interests

The authors declare having no conflict of interests.

Acknowledgments

The authors wish to acknowledge the Portuguese Foundation for Science and Technology (FCT) for the human resources grants: PhD grant BD/103571/2014 (EF), SFRH/BD/111242/2015 (AP), and FCT auxiliary researcher grant CEECIND/03186/2017 (JF). FCT is co-financed by European Social Fund (ESF) under Human Potential Operation Programme (POPH) from National Strategic Reference Framework (NSRF). The authors also acknowledge FCT the funding for CI-IPOP research unit (PEst-OE/SAU/UI0776/201), the Portuguese Oncology Institute of Porto Research Centre (CI-IPOP-29-2014; CI-IPOP-58-2015) and PhD Programs in Biomedicine and Pathology and Molecular Genetics of ICBAS-University of Porto. The

authors EF, DF and MR also acknowledge the financial support of the Research Group of Digestive Cancers (GICD) and the “Early stage cancer treatment, driven by context of molecular imaging (ESTIMA)” framework (NORTE-01-0145-FEDER-000027) and IPO-Score (DSAIPA/DS/0042/2018) for financial support. This article is also a result of the project NORTE-01-0145-FEDER-000012, supported by Norte Portugal Regional Operational Programme (NORTE 2020), under the PORTUGAL 2020 Partnership Agreement, through the European Regional Development Fund (ERDF). This work was financed by FEDER - Fundo Europeu de Desenvolvimento Regional funds through the COMPETE 2020 - Operacional Programme for Competitiveness and Internationalisation (POCI), Portugal 2020, and by Portuguese funds through FCT - Fundação para a Ciência e a Tecnologia/Ministério da Ciência, Tecnologia e Ensino Superior in the framework of the project "Institute for Research and Innovation in Health Sciences" (POCI-01-0145-FEDER-007274)

References

Adjei, I.M., Temples, M.N., Brown, S.B., Sharma, B., 2018. Targeted Nanomedicine to Treat Bone Metastasis. Pharmaceutics 10.

Azevedo, R., Peixoto, A., Gaiteiro, C., Fernandes, E., Neves, M., Lima, L., Santos, L.L., Ferreira, J.A., 2017. Over forty years of bladder cancer glycobiology: Where do glycans stand facing precision oncology? Oncotarget 8, 91734-91764.

Blanas, A., Sahasrabudhe, N.M., Rodriguez, E., van Kooyk, Y., van Vliet, S.J., 2018. Fucosylated Antigens in Cancer: An Alliance toward Tumor Progression, Metastasis, and Resistance to Chemotherapy. Front Oncol 8, 39.

Carrascal, M.A., Talina, C., Borralho, P., Goncalo Mineiro, A., Henriques, A.R., Pen, C., Martins, M., Braga, S., Sackstein, R., Videira, P.A., 2018. Staining of E-selectin ligands on paraffin-embedded sections of tumor tissue. BMC Cancer 18, 495.

Dominguez-Rios, R., Sanchez-Ramirez, D.R., Ruiz-Saray, K., Oceguera-Basurto, P.E., Almada, M., Juarez, J., Zepeda-Moreno, A., Del Toro-Arreola, A., Topete, A., Daneri-Navarro, A., 2019. Cisplatin-loaded PLGA nanoparticles for HER2 targeted ovarian cancer therapy. Colloids Surf B Biointerfaces 178, 199-207.

Duarte, H.O., Balmana, M., Mereiter, S., Osorio, H., Gomes, J., Reis, C.A., 2017. Gastric Cancer Cell Glycosylation as a Modulator of the ErbB2 Oncogenic Receptor. Int J Mol Sci 18.

El-Hammadi, M.M., Delgado, A.V., Melguizo, C., Prados, J.C., Arias, J.L., 2017. Folic acid-decorated and PEGylated PLGA nanoparticles for improving the antitumour activity of 5-fluorouracil. Int J Pharm 516, 61-70.

Engle, D.D., Tiriac, H., Rivera, K.D., Pommier, A., Whalen, S., Oni, T.E., Alagesan, B., Lee, E.J., Yao, M.A., Lucito, M.S., Spielman, B., Da Silva, B., Schoepfer, C., Wright, K., Creighton, B., Afinowicz, L., Yu, K.H., Grutzmann, R., Aust, D., Gimotty, P.A., Pollard, K.S., Hruban, R.H., Goggins, M.G., Pilarsky, C., Park, Y., Pappin, D.J.,

Hollingsworth, M.A., Tuveson, D.A., 2019. The glycan CA19-9 promotes pancreatitis and pancreatic cancer in mice. Science 364, 1156-1162.
Fernandes, E., Ferreira, J.A., Andreia, P., Luis, L., Barroso, S., Sarmento, B., Santos, L.L., 2015. New trends in guided nanotherapies for digestive cancers: A systematic review. J Control Release 209, 288-307.
Ferreira, J.A., Magalhaes, A., Gomes, J., Peixoto, A., Gaiteiro, C., Fernandes, E., Santos, L.L., Reis, C.A., 2017. Protein glycosylation in gastric and colorectal cancers: Toward cancer detection and targeted therapeutics. Cancer Lett 387, 32-45.
Ferreira, J.A., Peixoto, A., Neves, M., Gaiteiro, C., Reis, C.A., Assaraf, Y.G., Santos, L.L., 2016. Mechanisms of cisplatin resistance and targeting of cancer stem cells: Adding glycosylation to the equation. Drug Resist Updat 24, 34-54.
Fessi, H., Puisieux, F., Devissaguet, J.P., Ammoury, N., Benita, S., 1989. Nanocapsule formation by interfacial polymer deposition following solvent displacement. International Journal of Pharmaceutics 55, R1-R4.
Fry, L.C., Monkemuller, K., Malfertheiner, P., 2008. Molecular markers of pancreatic cancer: development and clinical relevance. Langenbecks Arch Surg 393, 883-890.
Golombek, S.K., May, J.N., Theek, B., Appold, L., Drude, N., Kiessling, F., Lammers, T., 2018. Tumor targeting via EPR: Strategies to enhance patient responses. Adv Drug Deliv Rev 130, 17-38.
Gomes, M.J., Kennedy, P.J., Martins, S., Sarmento, B., 2017. Delivery of siRNA silencing P-gp in peptide-functionalized nanoparticles causes efflux modulation at the blood-brain barrier. Nanomedicine (Lond) 12, 1385-1399.
Greish, K., 2007. Enhanced permeability and retention of macromolecular drugs in solid tumors: a royal gate for targeted anticancer nanomedicines. J Drug Target 15, 457-464.
Gupta, V., Trivedi, P., 2018. Chapter 15 - In vitro and in vivo characterization of pharmaceutical topical nanocarriers containing anticancer drugs for skin cancer treatment, in: Grumezescu, A.M. (Ed.), Lipid Nanocarriers for Drug Targeting. William Andrew Publishing, pp. 563-627.
Han, X., Yang, D., Yang, C., Spintzyk, S., Scheideler, L., Li, P., Li, D., Geis-Gerstorfer, J., Rupp, F., 2019. Carbon Fiber Reinforced PEEK Composites Based on 3D-Printing Technology for Orthopedic and Dental Applications. J Clin Med 8.
Hermann, N., Dressen, K., Schroeder, L., Debald, M., Schildberg, F.A., Walgenbach-Bruenagel, G., Hettwer, K., Uhlig, S., Kuhn, W., Hartmann, G., Holdenrieder, S., 2017. Diagnostic relevance of a novel multiplex immunoassay panel in breast cancer. Tumour Biol 39, 1010428317711381.
Hughes, J.M., Budd, P.M., Grieve, A., Dutta, P., Tiede, K., Lewis, J., 2015. Highly monodisperse, lanthanide-containing polystyrene nanoparticles as potential standard reference materials for environmental “nano” fate analysis. Journal of Applied Polymer Science 132.
Jeschke, U., Mylonas, I., Shabani, N., Kunert-Keil, C., Schindlbeck, C., Gerber, B., Friese, K., 2005. Expression of sialyl lewis X, sialyl Lewis A, E-cadherin and cathepsin-D in human breast cancer: immunohistochemical analysis in mammary carcinoma in situ, invasive carcinomas and their lymph node metastasis. Anticancer Res 25, 1615-1622.
Kalepu, S., Nekkanti, V., 2015. Insoluble drug delivery strategies: review of recent advances and business prospects. Acta Pharm Sin B 5, 442-453.
Kannagi, R., Izawa, M., Koike, T., Miyazaki, K., Kimura, N., 2004. Carbohydrate-mediated cell adhesion in cancer metastasis and angiogenesis. Cancer Sci 95, 377-384.

Kennedy, P.J., Sousa, F., Ferreira, D., Pereira, C., Nestor, M., Oliveira, C., Granja, P.L., Sarmento, B., 2018. Fab-conjugated PLGA nanoparticles effectively target cancer cells expressing human CD44v6. Acta Biomater 81, 208-218.

Konno, A., Hoshino, Y., Terashima, S., Motoki, R., Kawaguchi, T., 2002. Carbohydrate expression profile of colorectal cancer cells is relevant to metastatic pattern and prognosis. Clin Exp Metastasis 19, 61-70.

Lange, T., Valentiner, U., Wicklein, D., Maar, H., Labitzky, V., Brauns, A.-K., Streichert, T., Otto, B., Sauter, G., Wolters-Eisfeld, G., Riecken, K., Â¶rnchen, C.B., Kiefmann, R., Abraham, V., DeLisser, H.M., Gemoll, T., Habermann, J.K., Schumacher, U., 2016. E-selectin ligand binding affinity to determine anti-metastatic efficacy of proteasome inhibition. Journal of Clinical Oncology 34, e23010-e23010.

Marin, J.J., Al-Abdulla, R., Lozano, E., Briz, O., Bujanda, L., Banales, J.M., Macias, R.I., 2016. Mechanisms of Resistance to Chemotherapy in Gastric Cancer. Anticancer Agents Med Chem 16, 318-334.

Martins, C., Sousa, F., Araujo, F., Sarmento, B., 2018. Functionalizing PLGA and PLGA Derivatives for Drug Delivery and Tissue Regeneration Applications. Adv Healthc Mater 7.

Matsumura, Y., Maeda, H., 1986. A new concept for macromolecular therapeutics in cancer chemotherapy: mechanism of tumoritropic accumulation of proteins and the antitumor agent smancs. Cancer Res 46, 6387-6392.

Mereiter, S., Balmana, M., Gomes, J., Magalhaes, A., Reis, C.A., 2016. Glycomic Approaches for the Discovery of Targets in Gastrointestinal Cancer. Front Oncol 6, 55.

Pang, X., Li, H., Guan, F., Li, X., 2018. Multiple Roles of Glycans in Hematological Malignancies. Front Oncol 8, 364.

Park, S.C., Chun, H.J., 2013. Chemotherapy for advanced gastric cancer: review and update of current practices. Gut Liver 7, 385-393.

Pathan, N., Aime-Sempe, C., Kitada, S., Haldar, S., Reed, J.C., 2001. Microtubule-targeting drugs induce Bcl-2 phosphorylation and association with Pin1. Neoplasia 3, 70-79.

Patra, J.K., Das, G., Fraceto, L.F., Campos, E.V.R., Rodriguez-Torres, M.D.P., Acosta-Torres, L.S., Diaz-Torres, L.A., Grillo, R., Swamy, M.K., Sharma, S., Habtemariam, S., Shin, H.S., 2018. Nano based drug delivery systems: recent developments and future prospects. J Nanobiotechnology 16, 71.

Peixoto, A., Relvas-Santos, M., Azevedo, R., Santos, L.L., Ferreira, J.A., 2019. Protein Glycosylation and Tumor Microenvironment Alterations Driving Cancer Hallmarks. Front Oncol 9, 380.

Pereira, I., Sousa, F., Kennedy, P., Sarmento, B., 2018. Carcinoembryonic antigen-targeted nanoparticles potentiate the delivery of anticancer drugs to colorectal cancer cells. Int J Pharm 549, 397-403.

Pinho, S.S., Reis, C.A., 2015. Glycosylation in cancer: mechanisms and clinical implications. Nat Rev Cancer 15, 540-555.

Prokop, A., Davidson, J.M., 2008. Nanovehicular intracellular delivery systems. J Pharm Sci 97, 3518-3590.

Rawla, P., Barsouk, A., 2019. Epidemiology of gastric cancer: global trends, risk factors and prevention. Prz Gastroenterol 14, 26-38.

Salati, M., Di Emidio, K., Tarantino, V., Cascinu, S., 2017. Second-line treatments: moving towards an opportunity to improve survival in advanced gastric cancer? ESMO Open 2, e000206.

Samulitis, B.K., Pond, K.W., Pond, E., Cress, A.E., Patel, H., Wisner, L., Patel, C., Dorr, R.T., Landowski, T.H., 2015. Gemcitabine resistant pancreatic cancer cell lines

acquire an invasive phenotype with collateral hypersensitivity to histone deacetylase inhibitors. Cancer Biol Ther 16, 43-51.
Santos, J., Fernandes, E., Ferreira, J.A., Lima, L., Tavares, A., Peixoto, A., Parreira, B., Correia da Costa, J.M., Brindley, P.J., Lopes, C., Santos, L.L., 2014. P53 and cancer-associated sialylated glycans are surrogate markers of cancerization of the bladder associated with Schistosoma haematobium infection. PLoS Negl Trop Dis 8, e3329.
Sastre, J., Garcia-Saenz, J.A., Diaz-Rubio, E., 2006. Chemotherapy for gastric cancer. World J Gastroenterol 12, 204-213.
Scarpa, M., Noaro, G., Saadeh, L., Cavallin, F., Cagol, M., Alfieri, R., Plebani, M., Castoro, C., 2015. Esophageal cancer management: preoperative CA19.9 and CEA serum levels may identify occult advanced adenocarcinoma. World J Surg 39, 424-432.
Schultz, M.J., Swindall, A.F., Bellis, S.L., 2012. Regulation of the metastatic cell phenotype by sialylated glycans. Cancer Metastasis Rev 31, 501-518.
Senapati, S., Mahanta, A.K., Kumar, S., Maiti, P., 2018. Controlled drug delivery vehicles for cancer treatment and their performance. Signal Transduct Target Ther 3, 7.
Shen, H., Jawaid, A.M., Snee, P.T., 2009. Poly(ethylene glycol) carbodiimide coupling reagents for the biological and chemical functionalization of water-soluble nanoparticles. ACS Nano 3, 915-923.
Sousa, F., Cruz, A., Fonte, P., Pinto, I.M., Neves-Petersen, M.T., Sarmento, B., 2017. A new paradigm for antiangiogenic therapy through controlled release of bevacizumab from PLGA nanoparticles. Sci Rep 7, 3736.
Steinmetz, M.O., Prota, A.E., 2018. Microtubule-Targeting Agents: Strategies To Hijack the Cytoskeleton. Trends Cell Biol 28, 776-792.
Stiksma, J., Grootendorst, D.C., van der Linden, P.W., 2014. CA 19-9 as a marker in addition to CEA to monitor colorectal cancer. Clin Colorectal Cancer 13, 239-244.
Thorek, D.L.J., Elias, e.R., Tsourkas, A., 2009. Comparative Analysis of Nanoparticle-Antibody Conjugations: Carbodiimide Versus Click Chemistry. Molecular Imaging 8, 7290.2009.00021.
Trinchera, M., Aronica, A., Dall'Olio, F., 2017. Selectin Ligands Sialyl-Lewis a and Sialyl-Lewis x in Gastrointestinal Cancers. Biology (Basel) 6.
Vanderbeck, K., Voutsadakis, I.A., 2016. Elevation of Ca19-9 tumor antigen in colorectal cancer: an in silico investigation of pathogenesis. Int J Colorectal Dis 31, 1105-1107.
Wang, C., Li, X., Zhang, J., Ge, Z., Chen, H., Hu, J., 2018. EZH2 contributes to 5-FU resistance in gastric cancer by epigenetically suppressing FBXO32 expression. Onco Targets Ther 11, 7853-7864.
Zhang, C., Awasthi, N., Schwarz, M.A., Hinz, S., Schwarz, R.E., 2013. Superior antitumor activity of nanoparticle albumin-bound paclitaxel in experimental gastric cancer. PLoS One 8, e58037.
Zhang, N., Yin, Y., Xu, S.J., Chen, W.S., 2008. 5-Fluorouracil: mechanisms of resistance and reversal strategies. Molecules 13, 1551-1569.
Zhou, Y., Fukuda, T., Hang, Q., Hou, S., Isaji, T., Kameyama, A., Gu, J., 2017. Inhibition of fucosylation by 2-fluorofucose suppresses human liver cancer HepG2 cell proliferation and migration as well as tumor formation. Sci Rep 7, 11563.
Zhu, T., Hu, X., Wei, P., Shan, G., 2018. Molecular background of the regional lymph node metastasis of gastric cancer. Oncol Lett 15, 3409-3414.

Figure Captions

Figure 1. Transmission Electron Microscopy (TEM) analysis of 5-FU moAb functionalized PLGA-NPs **(A)** and Paclitaxel functionalized P-LGA NPs **(B)**. Scale bar represents 200nm.

Figure 2. FTIR analysis of functionalized NPs. Spectra of PLGA NPs showing a marked peak at 1750 cm^{-1} characteristic of PLGA (**A**); Spectra of PLGA-EDC/NHS NPs showing the no spectral alterations compared to PLGA NPs **(B)**; Spectra of PLGA-sLeA-NPs showing marked peaks at 1750 cm^{-1}, 1640 cm^{-1} and 1560 cm^{-1} vowing for the presence of carbonyl, amide and amine bonds corresponding to the covalent binding of anti-sLeA moAb to PLGA-NPs (**C)**.

Figure 3. Cumulative percentage release 5-FU **(A)** and Paclitaxel **(B)** from loaded PLGA-NPs throughout 72h at pH 7.4 (circle) and pH 3.5 (square). At any given timepoint, 5-FU-NPs released significantly higher amounts of cytotoxic drug at pH 7.4 than at 3.5, vowing for a pH-dependent release. Contrastingly, Paclitaxel release from PLGA-NPs was not pH-dependent in this experimental setup. Values are represented as a mean ± SD, n= 3. "****" $p < 0.0001$ (Kruskal–Wallis test)

Figure 4. Metabolic activity of gastric cancer cell lines AGS **(A, B)** and NCI-N-87 **(C, D)** after 24h exposure to 10, 50 and 100 nM free 5-FU and Paclitaxel or sLeA moAb functionalized loaded NPs. Empty functionalized NPs were added as negative control. The increase in concentration of free drugs was inversely correlated with cellular viability in both cell lines. AGS cells were more sensitive to 5-FU in comparison to paclitaxel whereas NCI-N-87 presented the opposite behaviour, denoting a cell-dependent drug response profile. Overall, AGS cells were more sensitive to the

citotoxic agents in comparison to NCI-N-87. Contrastingly, nanoencapsulation significantly reduced the toxicity profile of both drugs for the two cell lines. Values are represented as mean ± SD, n= 3. "**" $p < 0.01$; "***" $p < 0.001$; and "****" $p < 0.0001$ (Bonferroni' test)

Figure 5. Interactions of functionalized PLGA coumarin 6 (C6)- loaded NPs with gastric cancer cell lines (NCI-N-87 and AGS). Functionalized NPs (PLGAc-sLeA) showed a 2-fold increase in affinity for NCI-N-87 cells compared to void NPs (PLGAc), NPs with ECD/NHS linker (PLGAc- ECD/NHS) or functionalized with IgG1 isotype control (PLGAc-Isotype), as translated by the increased mean fluorescence intensity **(A, B)**, which was not observed in AGS cells **(A, C)**. Moreover, NCI-N-87 cells presented a higher uptake of functionalized NPs per cell in comparison to non-functionalized controls, while AGS cells showed no difference in internalization rates **(D)**.

Figure 6. Immunohistochemistry analysis of gastric cancer tissue sections using an anti-sLeA moAb **(A)** and sLeA functionalized PLGA-NPs (PLGA-sLeA NPs) **(B)**. Negative controls using empty PLGA NPs **(C)**, PLGA-EDC/NHS NPs **(D)** and PLGA-Isotype NPs **(E)** were run in parallel and showed no unspecific staining. High levels of sLeA were observed at the cell surface of tumour cells in advanced cases and corresponding metastasis **(F)** but not in the apparently normal adjacent mucosa (data not shown).

Figure 7. Immunohistochemistry analysis of healthy tissue sections from 9 relevant organs (stomach (**A**), liver **(B)**, skin **(C)**, lung **(D)**, kidney **(E)**, pancreas **(F)**, small intestine (**G**) and colon **(H)**) using PLGA-sLeA NPs. Functionalized NPs did not bind to leucocytes, muscle, stomach epithelium, liver or kidney sections. Low levels of staining were observed in pancreatic acini, superficial skin layers and in goblet cells.

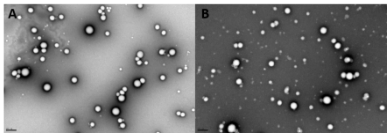

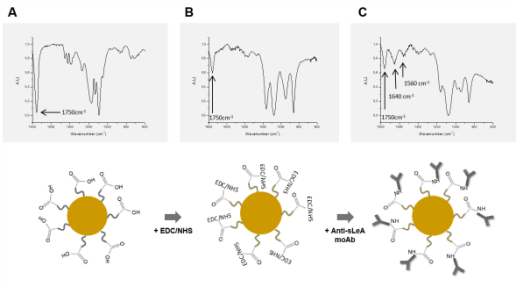

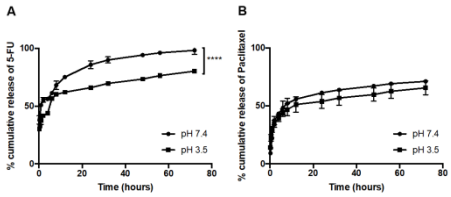

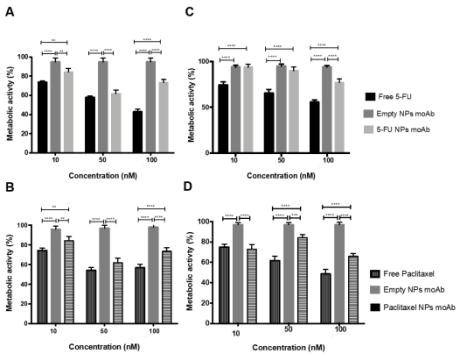

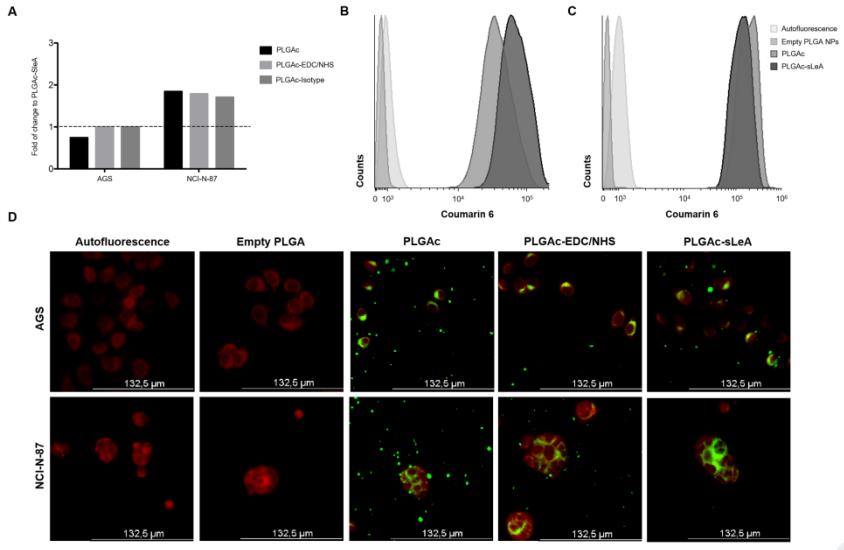

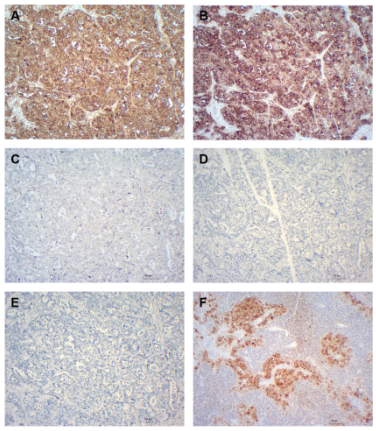

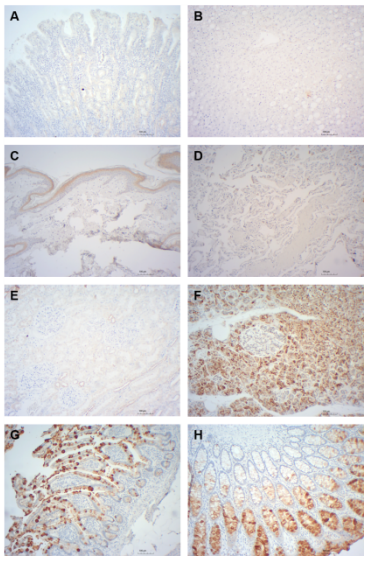

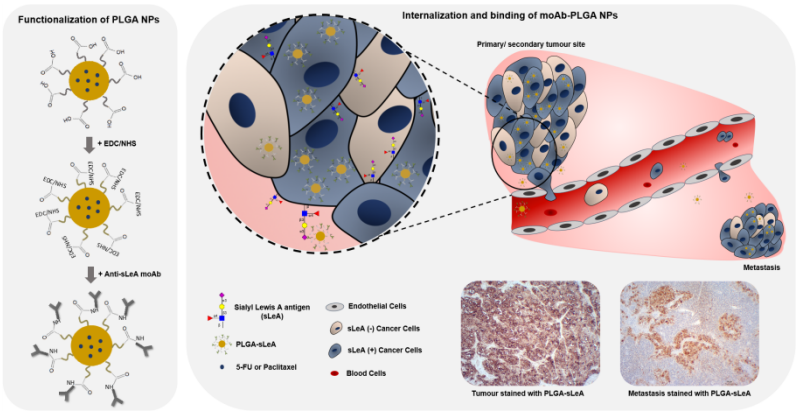

Conflict of interest

The authors declare having no conflict of interests.